Energy Engineering and Management, Vol. 13, No. 4, PP. 2-13, 2024

CFD Analysis of Ribs Effects on Heat Transfer in a Solar Parabolic Tough Collector

Mostafa Jamali[1], Najmeh Hajialigol[2*]

[1] Department of Mechanical Engineering, Hamedan University of Technology, Hamedan, Iran
jamali.mostafa79@gmail.com
[2] Department of Mechanical Engineering, Hamedan University of Technology, Hamedan, Iran
n.hajialigol@hut.ac.ir

Keywords:
solar parabolic collectors,
friction coefficient,
heat transfer,
Nusselt number,
Reynolds number,
numerical simulation,
CFD.

Original Research Article

Paper History:
Received: 27/02/2024
Revised: 17/04/2024
Accepted: 13/05/2024
Available online: 21/05/2024

Abstract: The production of electricity by solar thermal power plants is one of the promising ways to utilize renewable energy sources and reduce greenhouse gas emissions. Solar thermal power plants use concentrated solar radiation to heat a fluid that drives a turbine or an engine. One of the common technologies for concentrating solar radiation is the linear parabolic trough collector, which consists of a parabolic-shaped reflector that focuses the sunlight onto a receiver tube located at the focal line. In this research, the turbulent fluid flow and heat transfer in tubes with solid and porous fins as well as without fins were investigated numerically using a three-dimensional computational fluid dynamics (CFD) model. The objective was to study the impact of the fin type on the heat transfer and flow structure at different Reynolds numbers, which represent the ratio of the inertial forces to the viscous forces in the fluid. The findings showed that using the porous fin, the friction coefficient decreased and overall Nusselt number increased compared to the solid fin and the plain tube. The porous fin enhanced the heat transfer by creating more mixing and vortices in the fluid, while reducing the pressure drop by allowing some fluid to pass through the fin. The results of this research can provide useful insights for the design and optimization of internally finned tubes for solar thermal power plants.

How to cite this article: Jamali, M., Hajialigol, N., "CFD Analysis of Ribs Effects on Heat Transfer in a Solar Parabolic Tough Collector", Energy Engineering and Management, Vol. 13, No. 4, PP. 2-14, 2024. https://doi.org/10.22052/eem.2024.254462.1055

1. Introduction

Solar energy as an enormous energy resource can prepare a noteworthy portion of worldwide energy consumed [1-3]. Although much research has been conducted on the application of solar energy in solar thermal technologies, significant studies are still required to evaluate the issues and challenges related to these systems [4-7]. Concentrators are applied to convert solar energy into high-temperature heat in solar thermal energy technologies [8-10]. Parabolic trough solar collector is considered the most mature and the simplest technology among concentrated solar energy technologies for processes up to 400 °C with thermal oils [11] and up to 550 °C with molten salts [12].

Scholars have introduced a variety of analytical models aimed at enhancing the thermal efficiency of Parabolic Trough Collectors (PTCs). Ouagued [13] formulated a one-dimensional (1-D) model that factored in the working oil's role, dividing the Heat Collection Element (HCE) into multiple sections. Expanding upon this, Padilla [14] established control equations for glass, fluid, and absorber components. Both one-dimensional and two-dimensional (2-D) models were developed [15] with a key distinction being the division of the receiver into 'N' segments along the PTC's length in the 2-D model, as opposed to the 1-D model's approach. Discussions on these models included their underlying assumptions, constraints, and enhancement strategies along with the involved physical parameters.

Kalogirou [16] attempted simultaneous heat transfer through the glass cover and absorber pipe. Odeh's [17] model was capable of assessing the collector's efficacy based on the working fluids as it was predicated on the temperature of the absorber wall. Kassem [18] deduced that the heat transfer in PTCs could be adjusted by employing the right eccentricity, a finding derived from studying natural convection heat transfer between the absorber and the glass envelope. Gong [19] optimized the one-dimensional model and amalgamated it with a three-dimensional (3-D) end model, showcasing a strong correlation with empirical data. Lu [20] presented a non-uniform model that segregated the absorber and glass into regions with varying temperatures. The heat transfer dynamics were scrutinized using a combined method involving Monte Carlo Ray Trace and the Finite Volume Method [21]. Wu [22], in turn, pinpointed the non-uniform temperature distribution as a failure catalyst.

The primary objective behind developing these models was to boost PTC performance. Nonetheless, testing procedures prompted researchers to pivot towards analytical models due to one particular challenge. The computational duration is a significant aspect of modeling and thermal analysis with numerical methods often requiring months to finalize, given their dependency on Computational Fluid Dynamics (CFD) models. This has spurred extensive research into formulating analytical models that not only are simpler and faster but also surpass numerical methods in precision.

Cheng et al. [23] devised a model to examine the non-uniform temperature distribution within the receiver and the inconsistent solar flux incidence. This was achieved by bifurcating the setup into two dormant ends and two linear halves. Huang et al. [24] introduced a model that leveraged light distribution from reflective points to evaluate the PTC's optical efficiency. Behar et al. [25] investigated the impact of tracking modes on thermal efficiency, advocating for north-south and east-west orientations as the most effective. Ratzel et al. [26] engineered both analytical and numerical models to probe the heat dissipation through the receiver's annular space. They identified conduction and convection as the primary loss contributors and suggested curbing heat dissipation by using glass with minimal thermal conductivity and widening the annular gap between the envelope and the absorber tube.

A solar parabolic trough collector harnesses direct solar radiation, concentrating it along the collector's focal axis, which significantly raises the temperature of the heat transfer fluid. The PTSC system comprises a parabolic reflector that directs solar radiation onto a linear receiver positioned at its focus. By tracking the sun's movement, the collector ensures precise alignment of solar radiation with the receiver. The working fluid circulates through the receiver, absorbing the concentrated heat. The efficiency of PTCs hinges on several factors: the velocity of the fluid, the characteristics of internal heat gain, the geometric concentration ratio, and the rate of heat loss from the surface [27]. The design of the parabolic trough solar receiver is crucial to the system's overall efficacy. Studies indicate potential enhancements to PTCs performance, with studies spanning one-dimensional (1D), two-dimensional (2D), and three-dimensional (3D) analyses employing various computational fluid dynamics (CFD) techniques such as the finite volume method (FVM), boundary element method (BEM), finite element method (FEM), and finite difference method (FDM) [28].

Shuai et al. [29] utilized FEM and Monte Carlo ray tracing (MCRT) to model PTCs performance, revealing that radial stresses are minimal compared to axial stress. They observed that stainless steel and SiC exhibit higher radial stresses and temperature gradients than Cu and Al. Their findings also suggested that thermal stress could be reduced by 46.6% by using eccentric tube receivers. Tripathy et al. [30] investigated the material impact on a PTSC absorber tube using FVM, concluding that the heat transfer rate remains unaffected by the absorber tube's material. They discovered that Cu-Al-SiC-Fe and Cu-Fe composites could reduce maximum deflection by 45-49% and 7-15%, respectively, in comparison to steel. Kassem [31] applied FDM to estimate the convective heat transfer rate in the annulus between the glass cover and receiver of a parabolic-cylindrical solar collector. It deduces that optimal eccentricity selection could enhance heat transfer, thereby, decreasing the local Nusselt number with increased eccentricity.

Kumar et al. [32] examined the receiver tube alongside porous discs within a linear solar parabolic

trough collector, assessing the influence of receiver design, solar radiation concentration, and thermic fluid properties on heat collection. They reported that a receiver featuring a top porous disc configuration (where (w = di), (H = 0.5di), and (h = 30)) exhibited superior heat transfer capabilities, improving by approximately 64.3% with a pressure drop of 457 Pa compared to a standard tubular receiver. They also noted a significant enhancement in system performance due to the incorporation of porous media within tubular solar receivers.

Gunes et al. [33] conducted experimental research on pressure drop and heat transfer within a turbulent flow regime in a tube fitted with coiled wire inserts. Their studies indicated that coiled wire inserts markedly increased pressure drop and heat transfer compared to smooth tubes. Additionally, they found that the Nusselt number improved with thicker wires, higher Reynolds numbers, and lower pitch ratios. The most efficient overall enhancement, at 36.5%, was achieved with a wire characterized by (P/D = 1) and (a/D = 0.0892) at a Reynolds number of 3858.

Bellos et al. [34] posited that employing nanofluids, internal fins and a combination of these methods could boost thermal efficiency by 0.76%, 1.10%, and 1.54%, respectively. In subsequent research, Bellos et al. [35] explored the effects of reflective shields and internal longitudinal fins, finding that internal fins consistently yield thermal gains, while radiant shields prove beneficial at elevated temperatures.

Traditional PTCs focus solar radiation at the absorber tube's base, leading to deformation, thermal stress, and high temperatures. Norouzi et al. [36] suggested rotating the absorber tube at a specific frequency to mitigate high surface temperatures and to enhance solar energy absorption. They also experimented with a nanofluid (Al_2O_3-Therminol) as the heat-carrying fluid. Their proposed approximate 2D-transient model of PTCs and steady laminar numerical simulations for 3D scenarios showed that aluminum is the optimal material for the absorber tube, yielding an output temperature approximately 16 K higher—nearly 5% more than steel. This approach also resulted in a more uniform surface temperature distribution and improved the collector's thermal efficiency.

Enhancing heat transfer often involves increasing the effective heat transfer surface area, a common and effective strategy, despite the drawback of increased pressure drop. Utilizing guidance fins and porous media are two potent methods to augment the effective surface area and, thus, heat transfer [36]. Rashidi et al. [37] provided a thorough review of porous material applications in solar energy systems, while other studies have considered gradient porous properties to boost heat transfer with reduced pressure losses [38-40].

Viswanathan et al. [41] investigated turbulent flow in a fixed finned tube with a 180° bend using numerical methods, comparing the Detached Eddy Simulation (DES) model results with those of the Large Eddy Simulation (LES) model and experimental data. The DES model demonstrated a reasonable error margin relative to the LES model's numerical and experimental outcomes, which also reduced computation time significantly.

This research primarily aims to enhance the thermal efficiency of the parabolic trough solar collector receiver tube through the application of turbulent fins. Turbulent fins, a type of extended surface, improve the heat transfer coefficient and the Nusselt number for fluid flow within the tube. They also reduce pressure drop and drag force on the tube compared to plain or perforated fins. This study numerically investigates the turbulent fin geometry and its impact on flow and heat transfer characteristics, with anticipated results offering valuable insights for designing and optimizing parabolic trough solar collector receiver tubes equipped with turbulent fins.

2. Governing Equations and Boundary Conditions

The large eddy simulation was used in this study. The governing continuity, momentum, and energy equation were written as [42].

$$\frac{\partial}{\partial x_j}\left(\bar{\rho}\tilde{u}_j\right) = 0 \tag{1}$$

$$\frac{\partial}{\partial x_j}\left(\bar{\rho}\tilde{u}_i\tilde{u}_j\right) = -\frac{\partial \bar{P}}{\partial x_i}$$

$$\frac{\partial}{\partial x_j}\left(2(\bar{\mu}+\bar{\mu}_{SGS})\left[\tilde{S}_{ij}-\frac{1}{3}\delta_{ij}\tilde{S}_{kk}\right]\right) \tag{2}$$

$$\frac{\partial}{\partial x_j}\left(\bar{\rho}\tilde{u}_j\tilde{h}\right) = \frac{D\bar{P}}{Dt} + \frac{\partial}{\partial x_j}\left(\left(\frac{\bar{\mu}}{Pr}+\frac{\bar{\mu}_{SGS}}{Pr_t}\right)\frac{\partial \tilde{h}}{\partial x_j}\right) \tag{3}$$

$$\frac{\partial}{\partial x_j}\left(\bar{\rho}\tilde{u}_j k_{SGS}\right) - \frac{\partial}{\partial x_j}\left((\mu+\mu_{SGS})\frac{\partial k_{SGS}}{\partial x_j}\right) =$$

$$P_k - C_e\frac{\bar{\rho}k_{SGS}^{3/2}}{\Delta} \tag{4}$$

The modelling was carried out symmetrically due to the symmetrical shape of the solar collector, which was a cylinder with a length of 2 m. The walls, into which the heat flux entered, were divided into two parts. The upper surface was directly heated by radiation, but the heat flux of the lower surface was due to radiation caused by reflection.

The physical characteristics of the working fluid (water) were considered. The inlet velocity perpendicular to the surface is one of the boundary conditions of the inlet flow. The walls have a no-slip condition. A constant heat flux was considered to simulate the heating elements on the walls. The effect of wall roughness was ignored due to the insignificance of wall roughness compared to the presence of fin.

In the lower half of the receiver, the distribution of uniform heat flux is:

$$q'' = I_b C_R, r = \frac{D}{2}, -90 \le \theta \le 0, 0 \le L \le 2 \tag{5}$$

In the upper half of the receiver, the uniform heat flux distribution is:

$$q'' = I_g, r = \frac{D}{2}, 0 \le \theta \le 90, 0 \le L \le 2 \quad (6)$$

$$I_g = 750 W/m^2, I_b = 600 W/m^2$$

$$C_R = \frac{A_p}{A_r}$$

where C_R is the concentration ratio of the concentrator, I_b is the concentrated beam intensity, I_g is the intensity of the sun's radiation, A_r is the collector receiver area, and A_P is the collector concentrator area.

The friction coefficient of the tubes with solid and porous fins was calculated from Eq. 7.

$$f = \frac{\Delta p_e}{\rho U_m^2 / 2} \frac{D}{L} \quad (7)$$

where Δp_e is the effective pressure drop, and it is obtained from Eq. 8 in straight-finned tubes:

$$\Delta p_e = p_{in} - p_{out} + \frac{1}{2}\rho U_{in}^2 \quad - \frac{1}{2}\rho U_{out}^2 \quad (8)$$

$$U_{in} \quad = U_{out}$$

Eqs. 9 and 10 express the changes in the pressure drop and overall heat transfer coefficient in various mass fluxes for the tube with a porous trapezoidal fin.

$$h_f = \frac{q''}{T_{wall} - T_f} \quad (9)$$

$$Nu = \frac{h_f D_e}{k_f} \quad (10)$$

Finally, the thermal performance factor (TPF) represents the parameter that summarizes the thermal improvement and the increases in pressure drop compared to the reference case (smooth model) and provides details about the net energy gain of the system. This factor can be written as follows.

$$TPF = (\frac{Nu}{Nu_0})(\frac{f_0}{f})^{1/3} \quad (11)$$

3. Numerical Method and Validation

Fig. 1 displays a schematic of the solar collector geometry with trapezoidal fins. There are 84 fins in three rows of 28, and the distance between the fins is 66 mm. It should be noted that the fins were considered solid and porouslayout.

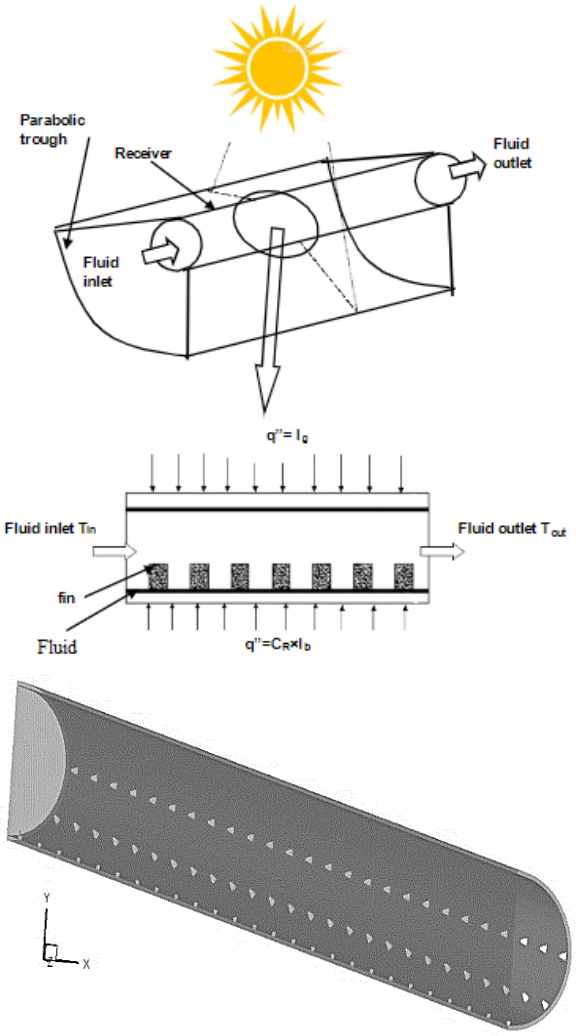

Fig. 1: Geometry of solar collector with trapezoidal fins

In the first step, the mesh quality function was checked. Then, the LES_IQ_k index was evaluated, defined as

$$LES\_IQ_k \quad = \frac{k^{res}}{k^{tot}} \quad (12)$$

Regarding the equations, k^{res} denotes the resolved kinetic energy, while k^{tot}represents the overall kinetic energy. Previous studies suggested that for high Reynolds numbers flows, an appropriate range be between 75% and 85% [42]. To determine a cost-effective and optimal mesh configuration, different grid sizes were evaluated.

For having an affordable and precise grid, various cell numbers were examined; finally, the cell number of about 1528000 was chosen.I n geometry with this number of cells LES_IQ_k is 0.91.

The geometric parameters of the receiver, the characteristics of the solid fin, the working fluid as well as the properties of the porous fin are given in Tables 1-3 respectively.

Table 1: Geometric parameters of the receiver and fin

Receiver inside diameter (mm)	D=66
Receiver length (mm)	L=2000
Square fin thickness (mm)	W=4
Distance between two fins (mm)	P=66
Trapezoidal shape fin (top and bottom thickness ratio)	λ=0.25

Table 2: Characteristics of the solid fins and the working fluid

Property	Working fluid	Solid fin
Density (kg/m^3)	938	8027
Specific heat (J/kg K)	1970	500
Thermal conductivity (W/m K)	0.118	20
Viscosity (N s/m^2)	0.000486	-

Table 3: Properties of the porous fins

Property	Porous fin
Porosity	φ=0.37
Permeability	K_p=2.9*10^{-10}

To verify the validity of the derived scientific model and the precision of the numerical outputs in the present study, it is necessary to correlate the previously reported results. In this research, the results of Reddy et al. [27] were used. The changes of Nusselt number in different mass flow rate for solid and porous trapezoidal tubes and comparison with numerical work of Reddy et al. can be seen in Figs. 2 and 3. The supreme variation between the results is less than 8%. Therefore, the current numerical procedure can capture the valid results.

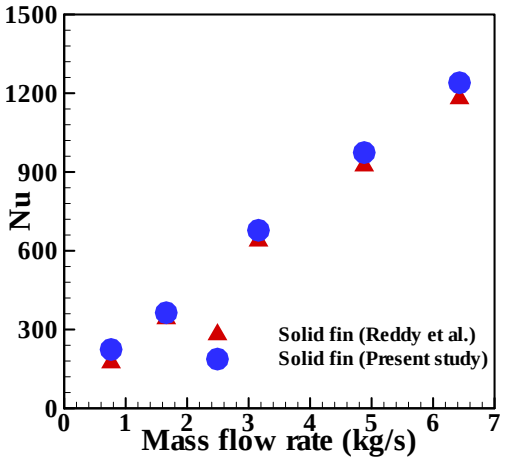

Fig. 2: Comparison of overall Nusselt number in different mass flow rate of solid trapezoidal tube with numerical results of Reddy et al [13]

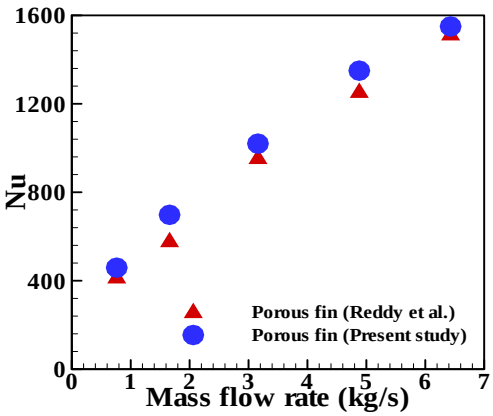

Fig. 3: Comparison of overall Nusselt number in different mass flow rate of porous trapezoidal tube with numerical results of Reddy et al [27]

4. Results and Discussion

The friction coefficient, a critical parameter in assessing the performance of collectors, is depicted in Fig. 4 for systems with solid and porous fins as well as those devoid of fins, across a spectrum of Reynolds numbers. Fig. 4 illustrates a trend where the friction coefficient diminishes as the Reynolds numbers escalate. This inverse relationship can be attributed to the enhanced inertia of the fluid at higher Reynolds numbers, which in turn reduces the frictional forces within the flow. The presence of fins particularly influences the friction coefficient. Utilizing fins in the design leads to a decrease in the friction coefficient, indicative of a smoother flow with less resistance. Notably, this reduction is more pronounced when porous fins are employed compared to the solid fins.

The porous fin's structure allows for a more distributed flow, reducing the resistance encountered by the fluid particles as they navigate through the collector. The porosity creates additional pathways, facilitating easier movement and lessening the impact of friction. Consequently, collectors with porous fins exhibit a lower friction coefficient, enhancing the system's efficiency by minimizing energy losses due to friction.

Moreover, the relationship between the friction coefficient and Reynolds numbers is not linear. At lower Reynolds numbers, the flow is predominantly laminar, and the friction coefficient is relatively high due to the viscous forces dominating the flow behavior. As the Reynolds number increases, transitioning the flow from laminar to turbulent, the inertial forces begin to outweigh the viscous forces, leading to a decrease in the friction coefficient. In turbulent flow, the chaotic and random motion of the fluid particles results in a lower net friction effect compared to laminar flow.

The design implications of these findings are significant. For instance, in applications where low friction is desirable to reduce pumping power and increase flow rates, porous fins may be a preferred choice. However, it is also essential to consider the potential increase in manufacturing complexity and cost

when opting for porous fins. The balance between performance enhancement and practical constraints must be carefully evaluated to determine the most suitable fin type for a given application.

Fig. 4 provides valuable insights into the fluid dynamics within collectors, highlighting the influence of fin design and Reynolds numbers on the friction coefficient. These insights are instrumental in optimizing collector designs for various industrial and commercial applications, ensuring efficient operation and energy utilization.

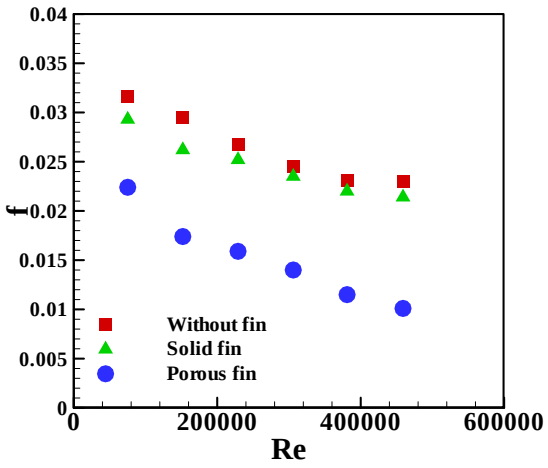

Fig. 4: Friction coefficient for tubes with solid and porous fins as well as without fins in different Reynolds numbers

Fig. 5 presents a comparative analysis of the average Nusselt numbers along the walls of tubes equipped with solid and porous fins as well as tubes without any fins. The data clearly indicates that the Nusselt number, which is a dimensionless representation of the convective heat transfer relative to conductive heat transfer across a boundary, escalates with a rise in Reynolds number. This trend is attributed to the fact that higher Reynolds numbers signify more turbulent flow conditions, which enhance the mixing of fluid and, thus, improve heat transfer efficiency. The incorporation of fins into the collector design amplifies the surface area available for heat transfer, which directly contributes to an increase in the Nusselt number. This is because the extended surface area provided by the fins allows more fluid particles to come into contact with the tube wall, thereby facilitating greater convective heat transfer. Porous fins, in particular, exhibit a more substantial increase in the Nusselt number compared to solid fins. The porous structure of these fins creates additional surface irregularities and channels for fluid flow, which disrupt the boundary layer more effectively and increase turbulence. This enhanced turbulence leads to a higher rate of convective heat transfer, which is quantitatively reflected in the increased Nusselt number.

Furthermore, the porosity of the fins introduces a myriad of tiny vortices within the flow as the fluid navigates through the porous matrix. These vortices serve to continually mix the fluid, bringing cooler fluid into contact with the heated surfaces and promoting a more uniform temperature distribution within the flow. This effect is particularly beneficial in applications where maintaining a consistent temperature profile is crucial. The implications of these findings are significant for the design and optimization of heat exchangers and solar collectors. By selecting the appropriate fin type—solid or porous—engineers can tailor the thermal performance of the system to meet specific requirements. For instance, in the situations where maximizing heat transfer is paramount, porous fins may be an optimal choice, despite potentially higher manufacturing costs and complexity. Fig. 5 underscores the importance of fin design in influencing the thermal performance of tubes in heat exchange systems. The insights gleaned from the figure can guide future advancements in collector technologies, paving the way for more efficient and effective thermal management solutions.

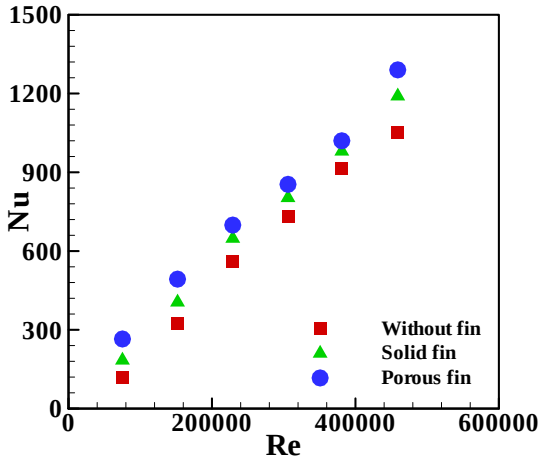

Fig. 5: Average values of Nusselt number on the tube walls for tubes with solid and porous fins as well as without fins.

Fig. 6 provides a detailed static temperature contour for a collector equipped with a porous fin at a Reynolds number of 50,000. The visualization captures the temperature distribution across the collector, highlighting the thermal dynamics at play. At the collector's inlet, where the boundary layer is initially the thickest, the temperature peaks. This is the result of the fluid's reduced velocity near the surface, which diminishes convective cooling and allows temperature to build up. As the fluid progresses along the collector, the boundary layer develops, and the temperature profile evolves. The highest heat transfer coefficients are observed in the regions immediately adjacent to the fins—both above and below. This is due to the disruption of the boundary layer by the fin's porous structure, which enhances the mixing of fluid layers and promotes more efficient heat transfer from the fluid to the fin surface and vice versa.

The porous fin's design plays a pivotal role in this process. Its permeability allows the fluid to penetrate into the fin, increasing the interaction between the fluid and the solid surfaces within the fin. This interaction is

crucial for convective heat transfer as it facilitates the exchange of thermal energy. The increased surface area provided by the porous fin also contributes to a higher heat transfer coefficient as there are more points of contact for the energy exchange. Moreover, the static temperature contour depicted in Fig. 6 can reveal the effectiveness of the fin design in terms of thermal distribution. A well-designed porous fin will create a more uniform temperature profile along the length of the collector, minimizing hot spots and ensuring that the heat transfer fluid is heated consistently. This uniformity is essential for the efficient operation of the collector, as it prevents areas of excessive heat that could lead to material stress or damage.

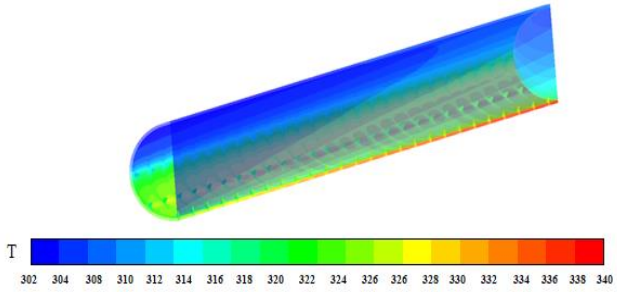

Fig. 6: Static temperature contour for a collector with a porous fi

Fig. 7 provides a visual representation of the temperature contours around the third fin in a collector, comparing scenarios with and without fins as well as with solid and porous fins at a Reynolds number of 50,000. The figure elucidates that the tube devoid of fins exhibits a lower temperature profile compared to its finned counterparts. This is primarily due to the absence of additional surface area for heat transfer that fins provide. In the case of tubes equipped with fins, there is a noticeable increase in temperature. This rise is attributed to the fluid's interaction with the fins, which disrupts the flow and creates longitudinal vortices. These vortices enhance the mixing of the fluid, thereby facilitating more effective heat transfer from the tube walls to the fluid. The solid fins, by virtue of their design, provide a substantial increase in the surface area in contact with the fluid, leading to improved heat transfer rates.

The tube featuring a porous fin, however, demonstrates an even greater increase in heat transfer as indicated by the higher fluid temperatures. The porous fin's structure allows for stronger secondary flows and more pronounced longitudinal vortices. These secondary flows are the result of the fluid's movement through the pores of the fin, which creates additional turbulence and mixing within the flow. The increased turbulence from these secondary flows and vortices leads to a more efficient disruption of the thermal boundary layer, allowing for a higher rate of convective heat transfer. Moreover, the porous fin's design inherently increases the effective heat transfer area beyond that of a solid fin. The multitude of pathways within the porous structure provides numerous points of contact for the fluid, significantly enhancing the heat transfer capabilities of the collector. As a result, the temperature of the fluid in contact with a porous fin is higher, indicating a more efficient transfer of thermal energy. The implications of these observations are profound for the design and operation of heat exchangers and collectors. By optimizing fin design, particularly through the use of porous materials, engineers can significantly improve the thermal performance of these systems. The increased efficiency not only leads to better energy utilization but also has the potential to reduce operational costs by minimizing the required input energy to achieve desired temperature levels.

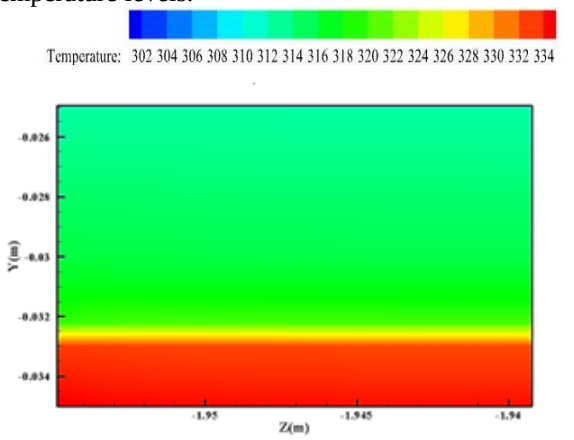

(a) Without fin

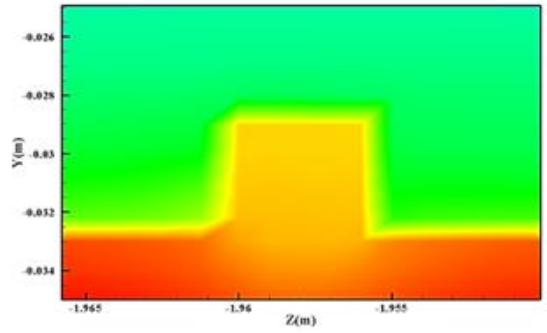

(b) Solid fin

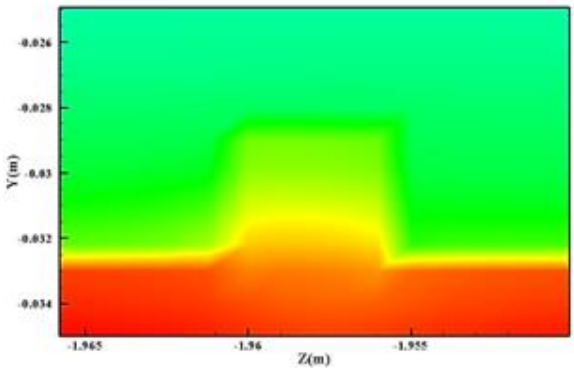

(c) Porous fin

Fig. 7: Comparison of temperature contour-Longitudinal section of the tube without fin and tubes with solid and porous fins

Fig. 8 delineates the variation in the Nusselt number for collectors under different conditions: without fins, with solid fins, and with porous fins, across varying mass flow rates and utilizing air and water as working fluids. The figure underscores a fundamental principle in heat transfer: as the mass flow rate increases, the rate of heat transfer does too. This is because a higher mass flow rate implies more fluid particles are available to carry away heat, enhancing the convective heat transfer process. The data reveals that the presence of fins significantly influences the Nusselt number. Collectors with solid fins exhibit a higher Nusselt number compared with those without fins, indicating an improved rate of heat transfer due to an increased surface area provided by the fins. This increase in surface area allows for more fluid contact, which facilitates greater convective heat transfer.

However, it is the porous fin that stands out in Fig. 8, achieving the highest Nusselt number among the cases examined. The porous structure of these fins introduces a complex network of channels, through which the fluid can flow greatly disrupting the boundary layer and enhancing the mixing of fluid layers. This results in a more effective convective heat transfer as evidenced by the elevated Nusselt number. When comparing the working fluids, water outperforms air, yielding a higher Nusselt number. Water's superior thermal properties, such as higher specific heat capacity and thermal conductivity, make it a more efficient heat transfer medium than air. Consequently, systems using water as the working fluid can achieve higher rates of heat transfer, which is advantageous in applications where thermal efficiency is critical. The implications of these observations are multifaceted. For engineers and designers, the insights from Fig. 8 can inform decisions on the optimal configuration of heat exchangers and collectors. In scenarios where high thermal efficiency is required, porous fins and water as a working fluid would be the preferred choices. However, these options may come with trade-offs such as increased material costs or system complexity

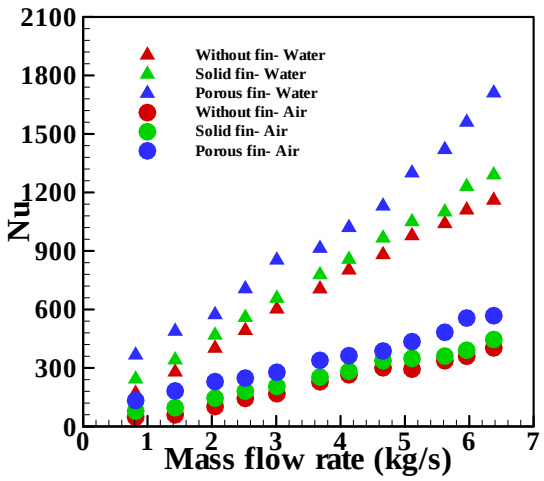

Fig. 8: Effect of the fin on the changes of Nusselt number in different mass rate for water and air

Fig. 9 illustrates the relationship between pressure drop and mass flow rate for a collector with a porous fin, using both water and air as working fluids. The figure indicates that as the mass flow rate increases, there is a corresponding increase in pressure drop. This is a fundamental principle in fluid dynamics: higher flow rates result in greater frictional forces within the system, which, in turn, causes a higher pressure drop. The comparison between water and air, as working fluids, reveals an interesting observation: the pressure drop for water is lower than that for air at equivalent mass flow rates. This can be attributed to the physical properties of the fluids—specifically density and viscosity. Water, being denser and more viscous than air, tends to exhibit a more streamlined flow, which can reduce the formation of turbulent eddies and vortices that contribute to pressure loss. Moreover, the porous fin's structure plays a role in the observed pressure drops. While the porosity enhances heat transfer by increasing turbulence, it also adds complexity to the flow path, which can contribute to pressure loss. However, the design of the porous fin can be optimized to strike a balance between increased heat transfer and manageable pressure drops. In practical applications, the choice of working fluid and the design of the fin must be carefully considered. Systems that prioritize energy efficiency may opt for water as a working fluid due to its lower pressure drop and superior heat transfer properties. Conversely, applications that require lower operational costs may choose air as a working fluid, accepting a higher-pressure drop-in exchange for the lower cost of air handling equipment.

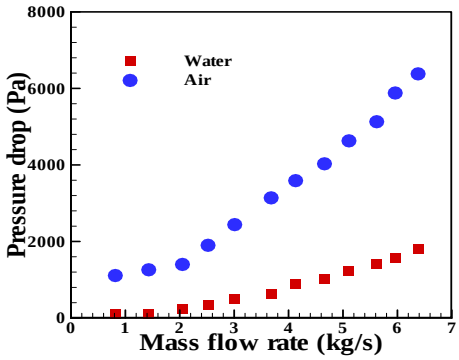

Fig. 9: Pressure drop for collector with porous fin in different mass rate for water and air

To delve deeper into the fin's impact on heat transfer, an examination of the heat transfer coefficient and of the local Nusselt number along the collector's length is essential. Fig. 10 and 11 showcase these parameters, revealing a distinct pattern. At the collector's inlet, the heat transfer coefficient and Nusselt number reach their zenith due to the pronounced temperature differential between the wall and the fluid, coupled with the slender thermal boundary layer. This scenario facilitates a robust heat exchange at the onset. As the fluid advances, encountering flow disturbances and instabilities, there is a marked escalation in the heat transfer rate. This surge is, however, short-lived as it diminishes with the weakening of the eddies and the reestablishment of the

thermal boundary layer. The passage through the first fin is a critical juncture; here, the boundary layer thickens, and the temperature gradient narrows, leading to a dip in the heat transfer coefficient and Nusselt number. This cyclical pattern of fluctuation is replicated as the fluid flows past the second and third fins. Each successive fin induces a similar response, but the magnitude of an increase in heat transfer is tempered by the diminishing strength of the eddies and the reduced temperature disparity between the fluid and the wall. Notably, the most significant heat transfer coefficient is observed in the regions immediately preceding and succeeding the fins. The dynamics of heat transfer in this context are complex. The fins serve as catalysts for disrupting the flow, thereby, enhancing the heat exchange. Yet, the very mechanism that amplifies heat transfer—the formation of eddies and flow instabilities—also leads to its subsequent reduction as the thermal boundary layer regrows. The presence of multiple fins along the collector's length ensures that the heat transfer process is not static but rather a dynamic interplay of fluctuating forces and thermal gradients. In essence, the heat transfer coefficient and local Nusselt number serve as indicators of the collector's thermal performance. Their variation along the length of the collector informs the design and optimization of finned systems, highlighting the need for a careful balance between fin-induced turbulence and the management of the thermal boundary layer. The ultimate goal is to harness the disruptive nature of the fins to maximize heat transfer while mitigating the effects of boundary layer growth and temperature homogenization. This delicate equilibrium is the key to enhancing the efficiency of heat exchange systems.

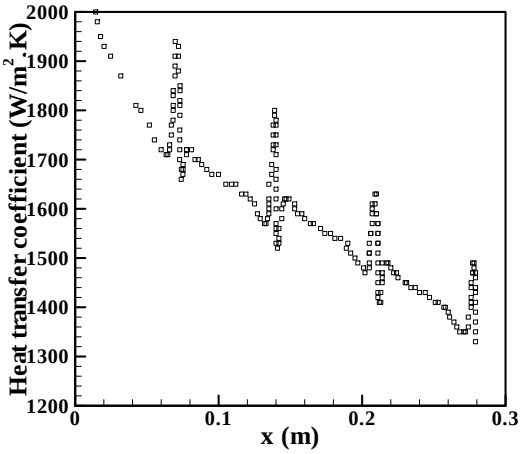

Fig. 10: Heat transfer coefficient along the collector

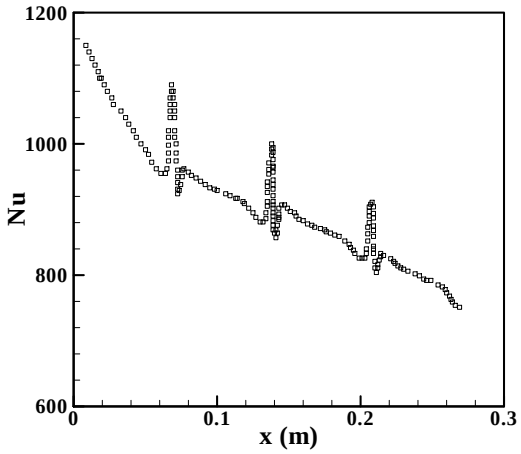

Fig. 11: Local Nusselt number along the collector

Fig. 12 offers a detailed examination of the average relative pressure changes across planes perpendicular to the flow axis at a Reynolds number of 60,000. The graph depicts a gradual decline in pressure along the flow path, attributable to the frictional drag exerted by the wall. This steady decrease represents the energy losses the fluid experiences due to its viscosity and the surface roughness of the collector's interior. As the flow encounters the first fin, there is a marked and abrupt drop in pressure. This sharp decline is the result of pressure drag, which occurs when the flow separates around the fin and creates a wake of low-pressure turbulence. The fin essentially acts as an obstacle, disrupting the flow and causing a significant local increase in energy dissipation.

Moving from the first to the second fin, the pressure reduction rate slows down considerably. This is indicative of the flow reestablishing itself after the disturbance caused by the first fin. However, upon reaching the second fin, the pressure plummets once again, albeit to a lesser extent than at the first fin. The reduced magnitude of this second drop can be linked to the fluid's loss of momentum, which diminishes the impact of subsequent fins on the flow. The pattern of pressure reduction observed at the third fin echoes that of the previous two, reinforcing the cyclical nature of pressure changes in the presence of multiple fins. Each fin introduces a new disruption to the flow, followed by a period of recovery where the pressure stabilizes before the next fin causes another drop. This cyclical pressure behavior has significant implications for the design and operation of finned collectors. Engineers must consider the balance between enhancing heat transfer through fin-induced turbulence and managing the associated pressure drops to maintain efficient fluid flow. The data from Fig. 12 is instrumental in optimizing fin spacing and geometry to achieve the desired thermal performance while minimizing energy losses due to pressure drag.

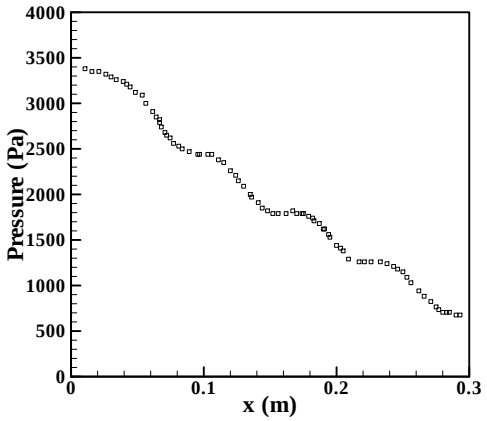

Fig. 12: Local pressure along the collector

Fig. 13 illustrates the relationship between thermal performance and the Reynolds number (Re) for collectors with different fin configurations. The trend indicates a decrease in thermal performance as Re increases for all types of fins. Specifically, a 20% reduction is observed for the collector without fins, while those collectors with solid and porous fins experience a 22% and 22.23% decrease in thermal performance, respectively, with changes in Re. The peak thermal performance values for collectors with porous, solid, and no fins are 1.4, 1.34, and 1.29 respectively, all occurring at a Reynolds number of 73,000. This convergence at a specific Re suggests that there is an optimal flow velocity—characterized by the Reynolds number—at which these collectors operate most efficiently.

The differences in thermal performance between the fin types are influenced by their ability to disrupt the flow and enhance heat transfer. Porous fins, with their complex structure, provide more surface area and create additional turbulence, which can improve heat transfer up to a point. However, as Re increases, the benefits of this turbulence are offset by the factors mentioned above. The findings from Fig. 13 are crucial for optimizing the design and the operation of thermal systems. They suggest that there is a need to balance the flow characteristics with the fin design to achieve the highest thermal performance. This balance is essential for developing efficient thermal management strategies in various applications, from industrial heat exchangers to solar collectors.

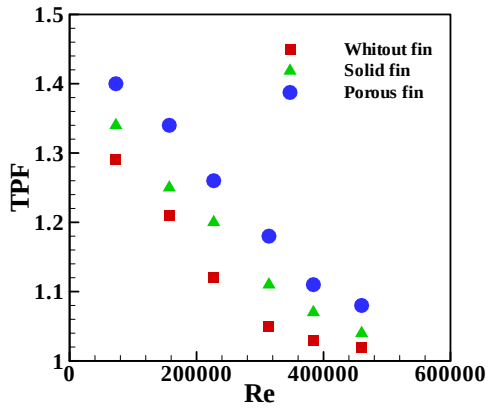

Fig. 13: Thermal performance with the considered range of the Reynolds number for tubes with solid and porous fins as well as without fins

5. Conclusion

This research delves into the intricate dynamics of turbulent fluid flow and heat transfer in collectors, focusing on configurations with solid fins, porous fins, and tubular receivers. The key findings from this study are as follows:

1. Mass Flow Rate and Heat Transfer: there is a direct correlation between the mass flow rate and the heat transfer coefficient; as one increases, so does the other. This relationship is more pronounced when water is used as the working fluid. Interestingly, the rate of an increase in the heat transfer coefficient diminishes as the mass flow rate continues to rise, indicating a form of diminishing returns at higher flow rates.
2. Pressure Drop Dynamics: similarly, the pressure drop within the collector escalates with an increase in mass flow rate. The graph depicting this relationship shows a steepening slope, suggesting that the pressure drop be more sensitive to changes in mass flow rate at higher values.
3. Fluid Type and Collector Efficiency: when comparing water-based and air-based fluids, the former exhibits superior performance, characterized by a higher heat transfer coefficient and a lower pressure drop. The increased mass transfer associated with water-based fluid flow enhances the collector's efficiency, as evidenced by the steeper slope of the heat transfer coefficient curve relative to the mass flow rate.
4. Porous Fin Advantages: the introduction of a porous fin into the collector system has been shown to decrease the friction coefficient while simultaneously increasing the Nusselt number. This improvement is notable when compared to systems with solid fins or no fins at all, underscoring the porous fin's efficacy in optimizing heat transfer.

Extending these findings, it becomes evident that the design of the collector's fin plays a pivotal role in its thermal performance. The porous fin, with its unique structure, not only facilitates better heat transfer but also mitigates frictional losses, which can be a significant advantage in high-flow scenarios. Moreover, the choice of working fluid is crucial; water's thermal properties make it a more effective medium for heat transfer compared to air, which can lead to more efficient collector designs. Future research could explore the long-term effects of these variables on collector performance, including the impact of fin wear and tear, fluid degradation, and the potential benefits of alternative working fluids. Additionally, the development of new materials for fins and working fluids could further enhance the efficiency and sustainability of collector systems. In conclusion, the insights gained from this study provide a foundation for the next generation of collector designs, emphasizing the importance of fin structure and fluid selection in achieving optimal thermal efficiency.

NOMENCLATURE

A_p	Aperture area of the solar trough collector, m^2
A_c	Receiver area, m^2
C_p	Isobaric specific heat, J/kg K)
C_R	Concentration ratio of the collector
d	Inner diameter of the receiver, m
D	Receiver outer diameter, m
D_c	Hydraulic diameter inside channel, m
D_o	Glass cover diameter, m
F	Form factor
Gr	Grashof number
h_ϵ	Heat transfer coefficient at inner surface of the receiver, W/ (m^2 K)
I_b	Beam radiation, W/m2
I_g	Global radiation, W/m2
k	Thermal conductivity, W/(m K)
K_p	Permeability, m2
L	Length of the receiver, m
l	Distance between two consecutive fins, m
Nu	Nusselt number
Pr	Prandtl number
Vp	Pressure drop per unit length of the receiver, kPa/m
Q_τ	Heat loss, W
P	Pressure of the fluid, N/m2
q"	Heat flux, W/m2
r	Radius, m
Ra	Rayleigh number
Re	Reynolds number
S	Magnitude of rate of strain
t	Thickness of the fin, m
T	Temperature, K
T_b	Outside bottom wall temperature of the receiver, K
T_i	Receiver surface temperature, K
T_o	Glass cover temperature, K
T_{o2l}	Receiver inside wall surface temperature, K
T_t	Outside top wall temperature of the receiver, K
u, v, w	Velocity of the fluid in x, y- and z-direction, $^m/_s$
U_{in}	Inlet velocity, m,s
x, y	Spatial position, m

Greek: Symbols

α_t	Inverse of Prandti number
α	Thermal diffusivity, $^{m^2}/_s$
β	Thermal coefficient of expansion, 1/K
ε	Turbulent dissipation rate, $^{m^2}/_{s^2}$
λ	Ratio of tip-to-base thickness of a fin, m
δ	Characteristics length, m
μ	Viscosity, $^{Ns}/_{s^2}$
υ	Kinematic viscosity of the fluid, $^{m^2}/_s$
φ	Porosity
ρ	Density, $^{kg}/_{m^2}$
θ	Angle, deg

Subscripts

Δ	Air
CF	Clear fluid
eff	Effective
f	Fluid
int	Interface
in	Inlet
Out	Outlet
PM	Porous medium
ref	Reference
s	Solid

References

[1] Kalogirou, S. A., "*Solar energy engineering: processes and systems*", Academic press, 2013.

[2] Almutairi, K., Nazari, M.A., Salem, M., Rashidi, M.M., Assad, M.E.H., Padmanaban, S., "*A review on applications of solar energy for preheating in power plants*", Alexandria Engineering Journal, Vol. 61, No. 7, pp. 5283-94, 2022, https://doi.org/10.1016/j.aej.2021.10.045.

[3] Verma, O.P., Manik, G., Sethi, S.K., "*A comprehensive review of renewable energy source on energy optimization of black liquor in MSE using steady and dynamic state modeling, simulation and control*", Renewable and sustainable energy reviews, Vol. 100, pp. 90-109, 2019, https://doi.org/10.1016/j.rser.2018.10.002.

[4] Yılmaz, İ.H., Söylemez, M.S., "*Design and computer simulation on multi-effect evaporation seawater desalination system using hybrid renewable energy sources in Turkey*", Desalination, Vol. 291, pp. 23-40, 2012, https://doi.org/10.1016/j.desal.2012.01.022.

[5] Hussein, A.K., "*Applications of nanotechnology in renewable energies—A comprehensive overview and understanding*", Renewable and Sustainable Energy Reviews, Vol. 42, pp. 460-76, 2015, https://doi.org/10.1016/j.rser.2014.10.027.

[6] Hussein, A.K.J.R, Reviews, S.E., "*Applications of nanotechnology to improve the performance of solar collectors*", Recent advances and overview, Vol. 62, pp. 767-92, 2016, https://doi.org/10.1016/j.rser.2016.04.050.

[7] Younis, O., Hussein, A.K., Attia, M.E.H., Rashid, F.L, Kolsi, L., Biswal, U., "*Hemispherical solar still: Recent advances and development*", Energy Reports, Vol. 8, pp. 8236-58, 2022, https://doi.org/10.1016/j.egyr.2022.06.037.

[8] El Ghazzani, B., Plaza, D.M., El Cadi, R.A., Ihlal, A., Abnay, B, Bouabid, K., "*Thermal plant based on parabolic trough collectors for industrial process heat generation in Morocco*", Renewable energy, Vol. 113, pp. 1261-75, 2017, https://doi.org/10.1016/j.renene.2017.06.063.

[9] Daabo, A.M., Ahmad, A., Mahmoud, S., Al-Dadah, R. K., "*Parametric analysis of small scale cavity receiver with optimum shape for solar powered closed Brayton cycle applications*", Applied Thermal Engineering, Vol. 122, pp. 626-41. 2017, https://doi.org/10.1016/j.applthermaleng.2017.03.093.

[10] Loni, R., Asli-Ardeh, E.A., Ghobadian, B., Kasaeian, A., "*Experimental study of carbon nano tube/oil nanofluid in dish concentrator using a cylindrical cavity receiver: Outdoor tests*", Energy Conversion and Management, Vol. 165, pp. 593-601, 2018, https://doi.org/10.1016/j.enconman.2018.03.079.

[11] Razmmand, F., Mehdipour, R., Mousavi, S.M., "*A numerical investigation on the effect of nanofluids on heat transfer of the solar parabolic trough collectors*", Applied Thermal Engineering, Vol. 152, pp. 624-33, 2019, https://doi.org/10.1016/j.applthermaleng.2019.02.118.

[12] Bonanos, A., Georgiou, M., Stokos, K., Papanicolas, C., "*Engineering aspects and thermal performance of molten salt transfer lines in solar power applications*", Applied Thermal Engineering, Vol. 154, pp. 294-301, 2019, https://doi.org/10.1016/j.applthermaleng.2019.03.091.

[13] Ouagued, M., Khellaf, A., Loukarfi, L., "*Estimation of the temperature, heat gain and heat loss by solar parabolic trough collector under Algerian climate using different*

thermal oils", Energ. Conver. Manage, Vol. 75, pp. 191–201, 2013, https://doi.org/10.1016/j.enconman.2013.06.011.

[14] Padilla, R.V., Gokmen, D., Goswami, Y., Stefanakos, E., Rahman, M.M., "*Heat transfer analysis of parabolic trough solar receiver*", Appl. Energy, Vol. 88, No. 12, pp. 5097–5110, 2011, https://doi.org/10.1016/j.apenergy.2011.07.012.

[15] Forristall, R., "*Heat transfer analysis and modeling of a parabolic trough solar receiver implemented in engineering equation solver*". No. NREL/TP-550-34169. National Renewable Energy Lab., Golden, CO.(US), 2003.

[16] Kalogirou, S.A., "*A detailed thermal model of a parabolic trough collector receiver*", Energy, Vol. 48, No. 1, pp. 298–306, 2012. https://doi.org/10.1016/j.energy.2012.06.023.

[17] Odeh, S.D., Morrison, G.L., Behnia, M., "*Modelling of parabolic trough direct steam generation solar collectors, Sol*." Energy, Vol. 62, pp. 395–406, 1998.

[18] Kassem, T., "*Numerical study of the natural convection process in the paraboliccylindrical solar collector*", Desalination, Vol. 209, No. 1–3, pp. 144–150, 2007, https://doi.org/10.1016/j.desal.2007.04.023.

[19] Gong, G., Huang, X., Wang, J., Hao, M., "*An optimized model and test of the China's first high temperature parabolic trough solar receiver*", Sol. Energy, Vol. 84, No. 12, pp. 2230–2245, 2020. https://doi.org/10.1016/j.solener.2010.08.003.

[20] Lu, J., Ding, J., Yang, J., Yang, X., "*Nonuniform heat transfer model and performance of parabolic trough solar receiver*", Energy, Vol. 59, pp. 666–675, 2013, https://doi.org/10.1016/j.energy.2013.07.052.

[21] He, Y.L., Xiao, J., Cheng, Z.D., Tao, Y.B., "*A MCRT and FVM coupled simulation method for energy conversion process in parabolic trough solar collector*", Renew. Energy, Vol. 36, No. 3, pp. 976–985, 2011, https://doi.org/10.1016/j.renene.2010.07.017.

[22] Cheng, Z.D., He, Y.L., Cui, F.Q., Xu, R.J., Tao Y.B., "*Numerical simulation of a parabolic trough solar collector with nonuniform solar flux conditions by coupling FVM and MCRT method*", Sol. Energy, Vol. 86, No. 6, pp. 1770–1784. 2012, https://doi.org/10.1016/j.solener.2012.02.039.

[23] Cheng, Z.D., He, Y.L., Qiu, Y.U., "*A detailed nonuniform thermal model of a parabolic trough solar receiver with two halves and two inactive ends*", Renew. Energy, Vol. 74, pp. 139–147, 2015, https://doi.org/10.1016/j.renene.2014.07.060.

[24] Huang, W., Peng, H.U., Chen, Z., "*Performance simulation of a parabolic trough solar collector*", Sol. Energy, Vol. 86, No. 2, pp. 746–755, 2012. https://doi.org/10.1016/j.solener.2011.11.018.

[25] Behar, O., Khellaf, A., Mohammedi, K., Ait-Kaci, S., "*Effect of Tracking Mode on the Performance of Parabolic Trough Solar Collector*", University of Bechar, 2013.

[26] Ratzel, A.C., Hickox, C.E., and Gartling, D.K., "*Techniques for reducing thermal conduction and natural convection heat losses in annular receiver geometries*", *J. Heat Transfer,* Vol. 101, No. 1, pp. 108-113, 1979, https://doi.org/10.1115/1.3450899.

[27] Reddy, K., Satyanarayana, G., "*Numerical study of porous finned receiver for solar parabolic trough concentrator*", Engineering applications of computational fluid mechanics, Vol. 2, pp. 172-84, 2008, https://doi.org/10.1080/19942060.2008.11015219.

[28] Bayareh, M., Usefian, A., "*Simulation of parabolic trough solar collectors using various discretization approaches: A review*", Engineering Analysis with Boundary Elements, Vol. 153, pp. 126-37, 2023, https://doi.org/10.1016/j.enganabound.2023.05.025.

[29] Shuai, Y., Wang, F.Q., Xia, X.L., Tan, H.P., "*Ray-thermal-structural coupled analysis of parabolic trough solar collector system*", ISBN, 2010.

[30] Tripathy, A. K., Ray, S., Sahoo, S.S., Chakrabarty, S., "*Structural analysis of absorber tube used in parabolic trough solar collector and effect of materials on its bending: A computational study*", Solar Energy, Vol. 163, pp. 471-85, 2018, https://doi.org/10.1016/j.solener.2018.02.028.

[31] Kassem T., "*Numerical study of the natural convection process in the parabolic-cylindrical solar collector*", Desalination, Vol. 209, No. 1-3, pp. 144-50, 2007, https://doi.org/10.1016/j.desal.2007.04.023.

[32] Kumar K. R., Reddy K., "*Thermal analysis of solar parabolic trough with porous disc receiver*", Applied energy, Vol. 86, No. 9, pp. 1804-12, 2009, https://doi.org/10.1016/j.apenergy.2008.11.007.

[33] Gunes, S., Ozceyhan, V., Buyukalaca, O., "*Heat transfer enhancement in a tube with equilateral triangle cross sectioned coiled wire inserts*", Experimental Thermal and Fluid Science, Vol. 34, No. 6, pp. 684-91, 2010, https://doi.org/10.1016/j.expthermflusci.2009.12.010.

[34] Bellos, E., Tzivanidis, C., Tsimpoukis, D., "E*nhancing the performance of parabolic trough collectors using nanofluids and turbulators*", Renewable and Sustainable Energy Reviews, Vol. 91, pp. 358-75, 2018, https://doi.org/10.1016/j.rser.2018.03.091.

[35] Bellos, E., Tzivanidis, C., "*Enhancing the performance of a parabolic trough collector with combined thermal and optical techniques*", Applied Thermal Engineering, Vol. 164, pp. 114496, 2020, https://doi.org/10.1016/j.applthermaleng.2019.114496.

[36] Norouzi, A.M., Siavashi, M., Oskouei, M.K., "*Efficiency enhancement of the parabolic trough solar collector using the rotating absorber tube and nanoparticles*", Renewable energy, Vol. 145, pp. 569-84, 2020, https://doi.org/10.1016/j.renene.2019.06.027.

[37] Rashidi, S., Esfahani, J. A., Rashidi, A., "*A review on the applications of porous materials in solar energy systems*", Renewable and Sustainable Energy Reviews, Vol. 73, pp. 1198-210, 2017, https://doi.org/10.1016/j.rser.2017.02.028.

[38] Wang, B., Hong, Y., Hou, X., Xu, Z., Wang, P., Fang, X., "*Numerical configuration design and investigation of heat transfer enhancement in pipes filled with gradient porous materials*", Energy Conversion and Management, Vol. 105, pp. 206-15, 2015, https://doi.org/10.1016/j.enconman.2015.07.064.

[39] Siavashi, M., Bahrami, H.R.T., "*Aminian E. Optimization of heat transfer enhancement and pumping power of a heat exchanger tube using nanofluid with gradient and multi-layered porous foams*, "Applied Thermal Engineering, Vol 138, pp. 465-74, 2018, https://doi.org/10.1016/j.applthermaleng.2018.04.066.

[40] Asiaei, S., Zadehkafi, A., Siavashi, M., "*Multi-layered porous foam effects on heat transfer and entropy generation of nanofluid mixed convection inside a two-sided lid-driven enclosure with internal heating*", Transport in Porous Media, Vol. 126, pp. 223-47, 2019, https://doi.org/10.1007/s11242-018-1166-3.

[41] Viswanathan, A. K., Tafti D. K., "*Detached eddy simulation of turbulent flow and heat transfer in a two-pass internal cooling duct*", International Journal of Heat and Fluid Flow, Vol. 27, No. 1, pp. 1-20, 2006, https://doi.org/10.1016/j.ijheatfluidflow.2005.07.002.

[42] Klein, M, "*An attempt to assess the quality of large eddy simulations in the context of implicit filtering. Flow*", Turbulence and Combustion, Vol. 75, No. 1-4, pp. 131-147, 2005, https://doi.org/10.1007/s10494-005-8581-6.